

# OPTICAL NETWORKS **FOR** EARTH-SPACE COMMUNICATIONS AND **THEIR** PERFORMANCE

**Kamran Shaik**  
Dennis **Wonica**  
Michael Wilhelm

Jet Propulsion Laboratory  
4800 Oak Grove Dr, Pasadena, CA 91109

## ABSTRACT

*This article **describes** optical subnets of ground based receiving stations for earth-space optical communications. The optical **subnet** concepts **presented** here provide full line-of-sight coverage of the ecliptic, 24 hours a day, with high weather availability. The technical characteristics of the optical station and **the** user **terminal** are presented as well as the **effects** of cloud cover, transmittance through the atmosphere, and impact of background noise for day or night time operation upon the communication link. In addition, candidate geographic sites are **identified**, and a link design for a hypothetical Pluto **mission** in 2015 is included.*

## 1. INTRODUCTION

Communications systems with higher carrier **frequencies** are **inherently** capable of operating at higher antenna gain and modulation bandwidth. Optical frequencies ( $\sim 10^{14}$  Hz) are several orders of magnitude higher than the operating carrier **frequencies** of the conventional radio frequency (RF) communication systems ( $\sim 10^{10}$  Hz) in use today. Optical systems promise smaller size and mass and lower power consumption as **compared** to RF systems with similar performance characteristics. For planetary space missions the advantage of **reduced** size, weight, and power **requirements** will allow more room for science instrumentation aboard a spacecraft.

The optical **subnet** concepts **investigated** for the Ground **Based** Advanced Technology Study (GBATS), and reported here are proposed as an augmentation to the deep space network (DSN), a network of antennas operated by the Jet Propulsion Laboratory (JPL) for NASA for communications with spacecraft. The GBATS study **was** performed in conjunction with the Deep Space Relay Satellite **S ystem** (DSRSS) study contracts<sup>1</sup> and its purpose was to initiate **study** of earth based **alternatives** to DSRSS in achieving significantly higher telemetry rates for future NASA deep space missions<sup>2</sup>.

The study of optical **subnets** draws upon previous design studies of the Deep Space Optical Reception Antenna<sup>3</sup> (DSORA) and work on a weather **model**<sup>4,5</sup> for ground based laser communications. **The** study also makes use of work accomplished by TRW, one of the contractors working on the DSRSS Study, for the user terminal design **concept**<sup>6</sup>. The emphasis of this work was on telemetry support. It is anticipated that future work will include **uplink** command, navigation, and optical **science**.

This report describes initial concept designs for **an** optical **subnet** as an augmentation to the DSN and their performance. In Section 2, a description of the ground optical terminal, which forms the basis of the optical **subnet**, and a description of the user spacecraft terminal are provided. An overview of the optical **subnet** concepts is provided in **Section** 3. The propagation and weather models are **developed** in Section 4 to provide a **basis** for the calculation of network availability and **coverage**. No specific planetary missions were considered in the design, though a hypothetical Pluto mission in 2015 is used as an illustration (see Section 4). Accordingly, future considerations of mission sets, operational issues, **enhancement** of the ground station's capabilities, etc., may profoundly affect the **performance**, configuration, and operation of an optical **subnet**.

## 2. GROUND AND SPACECRAFT OPTICAL TERMINALS

### 2.1 GROUND OPTICAL TERMINAL

Each Optical Station operates in the direct detection mode at optical wavelengths between 500 to 2000 nm. All calculations in this study were made using 532 nm as the operating wavelength. The telescope consists of a 10 m, non-diffraction limited, segmented primary mirror, and a secondary mirror, in a **Cassegrain** configuration as shown in Fig. 1. The telescope is mounted on azimuth-elevation gimbals and is housed in an environmental enclosure (dome). **The receiver subsystem** includes the beam reducer optics, staring mirror, tracking detector and the communications detector. Facilities for data processing, ground communications, logistics, security as well as office space, etc. are needed also, but are **not examined** in detail in this article.

The optical terminal as **described** in this section provides the basic building block of the optical **subnets**. The performance of the optical **subnets** calculated in the following sections of the report were based on the capabilities of a single ground station. The following assumptions and guidelines were used to arrive at a definition of the ground optical terminal.

- The optical terminal on ground is based on a 10 m diameter primary mirror
- **Telemetry** reception under both **daytime** and nighttime conditions
- Telemetry reception within 10 degrees of the sun
- Operating wavelength of 532 nm
- Tracking and slew rates compatible with deep space probes
- Acquisition of a user signal within 20 minutes at an elevation angle of about 15 degrees under all operating conditions
- A 2 mrad FOV for the **Cassegrain receiver** telescope with a coarse pointing accuracy of 0.2 mrad
- A 0.1 mrad FOV for the communications detector matching the blur diameter of the telescope
- A fine pointing mechanism with an accuracy of 0.01 mrad
- Station operation at high altitudes to **reduce** the impact of the atmosphere (up to 4.2 km)
- Uplink transmitter, command, emergency command, and navigation requirements were not considered at this time.

### 2.2 GROUND OPTICAL STATION BLOCK DIAGRAM

Fig.2 **describes the** flow of information and control signals for the receive **system** of the optical station. The **telescope** with a 10 m fast primary collects optical energy and delivers it to the **Cassegrain** focus. The Wide FOV sensor provides calibration, removes systematic telescope mount error, and **helps** in the acquisition of the user spacecraft within the telescope coarse FOV. From here the incoming beam is further reduced, controlled and delivered to the communications **detector**. The communications detector demodulates the optical signal and the resultant data stream is **fed** to the signal processor for bit/frame synchronization, decoding, error checking, etc. From the signal processor, the data is sent to the Ground Communications Facility (**GCF**) for transmission to the NOCC in real time. Raw or processed data is also stored in the archival subsystem for playback in case of GCF outage. The **executive** controller manages station activities automatically or manually through the command console, communicates with the outside world through the ground communications facility, and receives inputs from and sends commands to slave computers which include the pointing controller, the tracking **controller**, the figure controller, the signal processor, and the facility controller. For further details on the optical station architecture **see** ref. 2 and 3.

### 2.3 USER SPACECRAFT TERMINAL CONFIGURATION

The user configuration used in this study is based on a TRW concept for a future optical **terminal**<sup>7</sup>. Table 1 shows a list of important transmitter parameters and their **values** in this study to **estimate** telemetry capability. See Appendix A for further details on communications link parameters.

Table 1.  
Transmitter Parameters

Transmitter Parameter	Value
Average Power, W	7
Wavelength, nm	532
Aperture Size, m	0.75
Obscuration, m	0.0
Optics Efficiency	0.8
Pointing Bias Error, $\mu$ rad	0.1
RMS Pointing Jitter, $\mu$ rad	0.1

### 3. SUBNET OVERVIEW

#### 3.1 OPERATIONS CONCEPT

Like the current DSN, link geometry **drives** the major characteristics of the optical **subnet**. DSN users with interplanetary trajectories will require multiple stations located about the equatorial region to provide continuous **telemetry** support to any point near the ecliptic plane. As the earth rotates, continuous **telemetry coverage** is provided to any given user spacecraft via a hand-off strategy **between** the stations. As each station comes within the LOS of a user spacecraft and good **link** geometry is established, **telemetry** reception begins. As the earth continues **to** rotate and the user passes into the LOS of the next optical station, a hand-off occurs. Initial acquisition and tracking of a user spacecraft begins with the reception of the user **ephemeris** data provided by the DSN NoCC. The user **ephemeris** provides coarse pointing information to acquire the user transmit signal within the **field of view (FOV)** of the telescope. Once coarse pointing is established by identifying the received beam on the acquisition and tracking detector, the **receiver subsystem** uses a fast steering mirror for fine pointing and centering of the signal beam on the communications detector. User spacecraft tracking is maintained throughout the pass by the combined action of the coarse pointing mechanism of the telescope and the **fine** steering mirror. The acquisition **sequence** followed by **telemetry** reception is repeated with down line stations for the duration of the user need,

User pointing is established by detection of an **uplink** beacon, detection of the **crescent** earth, or detection of the sun with point ahead off-set to the earth (not part of the study). Coarse pointing is provided by the spacecraft attitude control system from data provided by an on-board **startracker**. Once the target (earth) is acquired within the FOV of the user telescope, a fast steering mirror fine points and **centers** the target on a **CCD** array. Data transmission begins once user pointing is established.

Based upon a 30 AU Pluto mission, and a 0.75 m user aperture, the footprint of the beam transmitted by the user **terminal** is smaller than the earth diameter, **therefore** it is necessary to point the beam to the designated receiving station(s) accurately. This can be accomplished since the pointing bias and jitter errors, as shown in the earlier section on the user terminal design, are much smaller than the signal beam diameter. A station is designated to receive telemetry when (i) it is within the LOS of the user terminal and that (ii) it has cloud **free** weather. The need to predict weather availability for some **subnet** configurations are addressed in appropriate sections below.

The baseline for this study provides for one **receive** aperture per geographic location. This places some restrictions on simultaneous support of multiple missions. For example, users with simultaneous coverage requirements must be located nominally 180 degrees apart.

#### 3.2 SUBNET CONFIGURATIONS

The presence of opaque clouds generally limits the availability of a single ground station for optical communications to less than 70 **percent**. This **problem** can be **handled** by employing spatial diversity.

There are two fundamentally different methods to provide the necessary spatial diversity to improve network weather availability for optical communications. The two concepts use different strategies in the location of optical stations to provide station diversity. These two approaches are **referred to as** the Clustered Optical **Subnet (COS)** concept and the **Linearly Dispersed Optical Subnet (LDOS)** concept. In this report, two specific configurations based on the COS and the LDOS concepts were **developed in detail**. They were a COS network with nine stations and an LDOS network with 6

stations. Both configurations were developed based upon site specific **weather** statistics, site surveys (literature search), coverage analysis, and projected telemetry performance. While using the same 10 m optical station and basic operations concept, each **subnet** offers unique advantages and disadvantages. Each **subnet** is designed to provide high weather availability. A detailed characterization of the two **concepts** and the reasons for selecting these numbers of stations are provided in Section 4.

It is **assumed** that each station will **require** less than 20 minutes to acquire, track and lock onto the incoming optical beam for both the LDOS and the COS concepts.

**Fig.3a** depicts network geometry for an LDOS showing **three** ground **stations**, and **Fig.3b** depicts geometry for a COS network showing two clusters with three stations each. **Telemetry** received by the available station for each **subnet** concept is demodulated and sent to the Station Data Processing **subsystem** for either processing and formatting, storage in the archival subsystem, or for transmission in raw form to **JPL's** Network Operations Control Center (**NOCC**) for distribution to **end** users. The stations are **connected** to the existing DSN infrastructure via the GCF.

#### 4. PERFORMANCE ANALYSIS

To develop optical network configurations that **meet** certain performance goals several analyses were performed to identify a preferred approach. These efforts **included the development** of a propagation model, a weather model, an ideal **coverage** model for the COS and the LDOS **concepts**, and availability assessments for various network configurations. For illustrative purposes two network configurations, one each from the COS and the LDOS concepts, were selected for detailed study. For these two configurations, an LDOS with six stations and a COS with three clusters of three stations (COS 3x3), a **coverage** analysis was made under ideal conditions **as well as a telemetry** performance projection for a Pluto mission in the year 2015.

##### 4.1 PROPAGATION MODEL

Earth's atmosphere has a dominating impact on the propagation model for ground based optical communications. Propagation loss and sky background radiance are two significant factors. Propagation loss or the transmittance of the atmosphere can be predicted using semi-empirical models under various operating conditions. The **problem** of opaque cloud cover is studied in **Section 4.2** where a weather model is produced.

The **U.S** Standard Atmosphere 1976 **was** used in this study to evaluate the effects of station altitude, meteorological range or visibility, and zenith angle, **Section 4.1.1** shows that the impact of using atmospheric models other than the U.S. Standard Atmosphere 1976 is very small.

It is **also** important to study the impact of sky background noise on optical communications, especially during the daytime operations. This is addressed in **Section 4.1.5**, where the **results** are used to develop average **telemetry** rates for daytime operations.

##### 4.1.1 Atmospheric Transmittance Model

LOWTRAN7, a transmittance model developed by Air Force **Geophysics** Laboratory (**AFGL**) for visible and infrared wavelengths, was used to calculate propagation effects on **wavelengths** of interest, including 532 nm. The **results** of using the US standard (1976), mid-latitude winter, and mid-latitude summer atmospheric models, on the transmittance, supplied with LOWTRAN7, are shown in **Fig.4a**. The curves shown for all the models assume the presence of high cirrus clouds, a 2.3 km altitude, a 17 km meteorological range or **visibility**, and a zenith path through the atmosphere. Since the atmospheric transmittance models do not differ significantly from each other, the US standard (1976) atmosphere was used to calculate nominal spectral transmittance under all operating conditions.

##### 4.1.2 Spectral Transmittance vs. Altitude.

**Fig. 4b** shows the transmittance for selected altitudes as predicted by **LOWTRAN7**. In the ideal **coverage** model, the station altitude (2.3 km) of the Table Mountain Facility (**TMF**) was used as the baseline for the optical stations.

Altitudes for the actual locations were used once specific LDOS and COS configurations were developed.

#### 4.1.3 Spectral Transmittance vs. Meteorological Range

Varying meteorological range or visibility will have an impact on the transmittance of the optical beam. Fig. 4c shows the spectral transmittance for **selected visibilities** for wavelengths **between** 0.4 and 2.0  $\mu\text{m}$ . A meteorological range of 17 km (defined as clear) was used as the basis for all calculations in this study.

#### 4.1.4 Spectral Transmittance vs. Zenith Angle.

The **most** dominant factor influencing the transmittance of the optical beam through the atmosphere is the operational zenith angle when receiving telemetry from the **spacecraft**. Fig. 4d is a LOWTRAN7 plot of spectral transmittance for **selected** zenith angles for wavelengths **between** 0.4 to 2.0  $\mu\text{m}$ . At 70° zenith angle, the air mass through which the signal must propagate is about three times larger than the air mass at zenith. This is equivalent to about 10 dB of loss. In this study, **telemetry reception** of the optical station down to a zenith angle of 70° is included in the **coverage** analysis and link calculations.

#### 4.1.5 optical Background

Optical communications system performance in terms of data rate varies significantly **between** night and day. For a ground based **receiver**, the sky radiance is a major source of optical noise, especially for **daytime** operation. This information was factored in when data volume over a 24 hour period was calculated for the GBATS study.

**4.1.5.1 1 ghitime** The sky brightness at night is about 5  $\text{nW}/(\text{m}^2 \cdot \text{nm} \cdot \text{sr})$ . This brightness is equivalent to a star of visual magnitude 21.25 per square **arcsecond**<sup>8</sup>.

**4.1 . 5 . 2 D - . Fig.5** shows sky radiance **as** a function of solar elongation, It **decreases** by an order of magnitude for solar elongation (sun-earth-spacecraft angle) of 180° from a high of about 0.6  $\text{W}/(\text{m}^2 \cdot \text{nm} \cdot \text{sr})$  when looking about 10° from the sun. The graph is derived from LOWTRAN7 calculations under normal weather (17 km visibility) for a TMF like receiver site. An averaged daytime data rate **was** calculated using six representative daytime sky radiances, specifically at 10, 40, 70, 100, 130, and 160 **degrec** solar elongation.

### 4.2 WEATHER MODEL AND AVAILABILITY ANALYSIS

Besides geometry, the **largest** driver in terms of network performance is weather availability. With optical communications the effects from weather on station availability are significantly more **severe** than at microwave **frequencies**. Unlike microwave **frequencies**, practically no communications can exist when the propagation path for an optical link is blocked by clouds. In this study, a weather model developed by **Shaik**<sup>9</sup> was used to model the effects on link availability for optical stations in spatially **independent** weather cells. A total network availability of 90% was chosen as the performance goal,

#### 4.2.1 Weather Model

For potential optical station sites, rough estimates of pertinent weather statistics can be obtained from existing sources which include weather satellites. **Fig.6** shows a contour diagram for the probability of clear sky over the United States obtained from 2 years of GOES satellite data<sup>10</sup>. As can be seen the probability of cloud free skies over the **southern** California is about 66 percent. This means that 34% of the time this area has partial to full cloud cover. To provide 90% or greater availability requires that multiple stations within the line of sight of the user spacecraft but located in different **uncorrelated cells** be employed.

Based upon **empirical** information obtained from the Air Force Geophysics Laboratory (AFGL), the cloud system correlation **coefficient between** sites was expressed as<sup>1</sup>

$$(1) \quad p = \exp[-\Delta x^2/2\sigma^2]$$

where  $\Delta x$  is the distance between sites and  $\sigma \approx 50$  km. This empirical result is then used to obtain the extent of cloud **system** correlation for any two sites. An inter-site distance of at least 3-4  $\sigma$  or about 150-200 km for  $p \leq 0.01$  is found adequate to ensure spatially independent weather **cells**.

Given ground stations in spatially independent weather cells, a parametric weather **model**<sup>12</sup> can be used to compute link availability statistics. The model may be used to predict joint probability (or the percentage of time) for which weather the extinction loss through the atmosphere is less than some threshold for at least one of the ground stations. Define  $\omega_n(L)$  as the cumulative distribution function (CDF) as the fraction of time when the propagation loss due to the atmosphere is less than or equal to  $L$  dB for at least one of the  $n$  sites with a LOS to the user **spacecraft**. The weather availability can then be expressed as the CDF,

$$(2) \quad \omega_n(L) = 1 - (q \exp[-0.23 b(L-L_0)])^n; (L \geq L_0)$$

where  $L_0$  is the acceptable loss through the atmosphere in dB, and defines the operational **telemetry line** for the optical **subnet**. The minimum loss through the atmosphere is given by  $\eta_a \sec(\zeta)$  in dB, where  $\zeta$  is the zenith angle and  $\eta_a$  represents a site altitude dependent empirically derived propagation loss through the atmosphere under normal clear conditions. Since  $\eta_a \sec(\zeta)$  estimates the minimum possible loss through the atmosphere,  $L_0 > \eta_a \sec(\zeta)$ . Parameter  $b$  is a site dependent parameter and is derived empirically to model the CDF curve<sup>13</sup>. In this study,  $b=0.1$ , and is derived from the assumption that  $w, (L=30)=0.8$  at zenith. The equation assumes that the probability of cloudy skies,  $q$ , is the same for all sites, but can be easily extended to site dependent  $q$ .

In the absence of site dependent empirical weather database, eq. (2) provides a simple model to compute the weather availability of an **optical subnet**. For example, under normal weather conditions for Table Mountain Facility (TMF), minimum propagation loss at  $\zeta=60^\circ$  is -4.7 dB. Choosing this as the acceptable propagation loss,  $L_0=-4.7$  dB, with  $q=0.34$  at TMF, the availability of a single site for  $L=L_0$  is found to be  $\omega_1(L_0)=0.66$ . If there are three such independent and identical sites in a **subnet** within the LO-S of the user, then from eq.(2), the **subnet** availability is found to be  $\omega_3(L_0)=0.96$ .

#### 4.2.2 Weather Availability.

Weather availability is a measure of station outage due to weather effects such as clouds, rain, and dense fog. Individual sites for an optical **subnet** are chosen for their good cloud free statistics, and are located far enough apart as indicated by eq. (1) to ensure independent weather from station to station. Availability of a single station is **expected** to be at least 66 percent. The availability of a given network configuration is discussed in Section 4.4.

### 4.3 COVERAGE ANALYSIS

LOS coverage (or simply coverage) is defined as the percent of time during a day when a straight line path between one or more than one stations at earth and the user spacecraft is present. All networks **considered** here must provide full **coverage**.

A ground-based network consists of earth stations strategically placed around the globe to provide full **coverage**, 24 hours a day. Ideally only two stations near the **equator** exactly  $180^\circ$  apart are required to provide full coverage. However, the number of stations quickly increases due to the constraint on the minimum elevation angle of  $15^\circ$ , the fact that the stations cannot be always placed at the equator, and the need to have more than one station in the spacecraft LOS to

provide high weather availability. Specific network configurations and the coverage they provide are presented in the following paragraphs.

#### 4.4 NETWORK ANALYSIS

The most promising **network** concepts which provide high weather availability and full **coverage** of the ecliptic were introduced in Section 3.2. In this section, **subnet concepts** are described in greater detail under idealized conditions to provide a rationale for the selection of promising configurations. **The selected** configurations, an LDOS with six stations, and a COS configuration with nine stations are then studied under realistic conditions with **reference** to a Pluto mission in 2015. The coverage curves and the **telemetry** rates are derived using **actual** site parameters including **longitude**, latitude, altitude, and the cloud cover statistics obtained from satellite data or *in situ* observations, and compared to the results obtained under ideal conditions.

##### 4.4.1 Analysis for Linearly Dispersed Optical Subnet (LDOS)

In this study, LDOS configurations were **designed** with 6-8 ground stations spaced roughly equidistant from each other, and placed around the globe near the equatorial region. An LDOS with 5 stations was not considered since the **availability** of this configuration is **considerably** below 90%, and because the optical **subnet** would need to operate at very low elevation angles for a large fraction of the time.

Since the characteristic cloud systems according to **eq. (1)** are of the order of a few hundred **kilometers in size**, much smaller than the inter-station distance, the adjacent stations will **lie** in different climatic regions and thus have **uncorrelated** cloud cover statistics. Once specific sites were chosen, single as **well** as joint cloud cover statistics for two or more consecutive sites were **evaluated** and used to predict link availability.

The probability of an outage for the LDOS configuration is **low** because (i) several stations are within the LOS of the user **spacecraft**, and (ii) the stations **lie** in different climatic zones and hence their weather patterns are **uncorrelated**. Since the receiving sites are far **apart**, data with high spatial resolution on cloud cover statistics is not **needed**. Existing data with a resolution of about 100 km is sufficient. However, **further** site surveys are needed to provide weather data with high temporal resolution. The weather data with high temporal resolution are **needed** to compute and predict short-term outage statistics accurately. Weather data with hourly or better temporal resolution will probably be needed to finalize site selection.

The distance between the receiving stations in the LDOS concept is very large, therefore, full benefit of using optical wavelengths can be **realized** only when the user spacecraft points accurately to the **designated receiving** station in the **subnet**. Since the spacecraft can be 4-5 light hours from the earth for some planetary missions, weather availability of the **subnet** has to be predicted several hours in advance to designate the receiving station and, the location of the designated station must be **uplinked** to the user terminal for pointing purposes.

**4.4.1.1 LDOS With Six Ground Stations.** The Linearly Dispersed Optical **Subnet (LDOS)** which consists of six optical stations located approximately 60 **degrees** apart about the equatorial region is shown in **Fig.7**. Each optical station is located in a different climatic region (approximately 7000 km apart) and thus **has** statistically **uncorrelated** cloud cover. The model assumes that all station sites have normal visibility (17 km) and are as high as the Table Mountain Facility (2.3 km) to reduce propagation loss. It is also **assumed** that each site has **at least** 66% cloud free days (i.e.  $q=0.34$ ).

**Fig.8** shows ideal coverage curves for six stations sixty degrees apart. For this configuration, only two stations will have a LOS coverage of the spacecraft at all times when the **telemetry** line used is consistent with a 60° zenith angle. The availability for this optical **subnet** is **calculated to be**  $\omega_2(l_0) = 0.88$ . The availability of the **subnet** can be **increased** to about 92 percent if a telemetry line consistent with 75° zenith angle can **be used**.

Consider the situation when station 3 is **receiving** from a spacecraft on an equatorial path. The natural point to hand-off **telemetry** to station 4 is when **zenith** angles  $\zeta_3 = \zeta_4 = 30^\circ$  (subscript refers to the station number). Note that while  $\zeta_3$  is increasing,  $\zeta_4$  is **decreasing**. As **calculated from** the weather model **described** above, about 12% of the time station-4 will be unavailable due to weather. In this case, station 3 continues to **receive** up to  $\zeta_3 = 60^\circ$ , at which point station 5 is

activated at  $\zeta_5=60^\circ$ . For this configuration, the logical place for the telemetry line (or acceptable zenith angle loss through the atmosphere) is at  $\zeta=60^\circ$ . This leaves about one hour for acquisition and overlap between stations, as the stations are required to operate down to  $\zeta=75^\circ$  in zenith.

Table 2 provides a list of possible **geographical** sites for this LDOS configuration as an example. Appendix B describes the guidelines and the procedures used to select **geographical** sites in this and the following site tables. Weather statistics for all locations, except for Hawaii and Chile sites, were obtained using satellite data<sup>14</sup> and are shown in Table 2. The data used for Hawaii and **Cerro Pachan** in Chile was based upon *in situ* observations<sup>15</sup>. Table B-1 in Appendix B lists possible additional sites.

Table 2  
Linearly Dispersed Optical Subnet with 6 Ground Optical Stations.

	Location	Altitude km	Longi- tude	Latitude	Time Zone	cloud free days/ Weather	Notes
1	SouthWest United States Table Mt. Facility, Ca.	2.3	118 W	34 N	-8	66%/arid[1]	[3]
2	Hawaii, USA Mauna Kea	4.2	155 W	20 N	-10	>69%/dry[2]	[3]
3	Australia Siding Spring Mt.	1.1	149 E	31 s	+10	67%/dry	[3]
4	Pakistan Ziarat	2,0	68 E	30 N	+5	69%/arid	[4]
5	Spain/NorthWest Africa Calar Alto, Spain	2.2	2W	37 N	-1	67%/arid	[3]
6	S. America Cerro Pachan, Chile	2.7	71 w	30 s	-4	77%/arid[2]	[3]

[1] ISCCP satellite data; [2] The NOAO 8-M Telescopes proposal to NSF; [3] Preexisting facilities and infrastructure [4] Information on infrastructure and facilities not available

Using specific sites given in Table 2 and assuming a hypothetical mission to Pluto in 2015 for illustrative purposes, a set of **coverage** curves were **derived** for a realistic LDOS with six stations. **Fig.9** shows the coverage curves when data on actual geographical sites is used for the Pluto mission. The site specific information used to obtain these curves includes altitude, longitude, latitude, as well as Pluto's trajectory across the sky. Note that Pluto does not pass through the zenith for any of the sites. As can be seen in the figure, coverage will last from 2.5 to 4 hours depending on the specific latitude of the optical station. For example, the site in Siding Spring Mt., Australia, a **telemetry** pass will last approximately 4 hours.

A close examination of Fig.9 shows that the **telemetry** curve has been placed a little lower compared to **Fig.8**. The acceptable atmospheric loss for the realistic Pluto mission is about -6.2 dB instead of -4.7 dB for the ideal case. This was a consequence of the fact that the exact locations of the real sites were situated away from the equator. Even then the time for which 3 stations are available at greater than  $15^\circ$  above the horizon has been **reduced** to about 7 hours from 12 hours under the generic **case**. These adjustments have reduced the network availability for LDOS with six stations to about **91%**. Also note that the acquisition time is about 20 minutes for the Pluto mission case instead of 1 hour for the ideal case.

**4.4.1.2 LDOS With Seven Ground Stations.** The inter-station distance in this case will be roughly  $51''$  in longitude ( $\sim 6000$  km). Here, **35 percent** of the time **three** stations will be 30 or more **degrees** above the horizon. The rest of the time only two stations will be available. When two or three stations are **within** the LOS, the availability is calculated to be  $w_{2/3}(L_0)=0.65 w_2(L_0)+0.35 w_3(L_0)=0.91$ . The **telemetry** line for this configuration is at  $60^\circ$  zenith angle,

**4.4.1.3 LDOS With Eight Ground Stations.** The inter-station distance for this configuration will be roughly  $45^\circ$  in longitude ( $\sim 5000$  km). This configuration will ensure that three stations are 30 or more **degrees** above the horizon about **66 percent** of the time in a day. An LDOS with 8 stations will provide 94% availability. The **telemetry** line will be at  $60^\circ$  zenith angle as before, providing considerably long overlap between stations.



#### 4.4.2 Analysis for Clustered Optical Subnet (COS)

For geopolitical or operational reasons the stations of an optical subnet may be required to be located within three or four locations around the globe, chosen for their optimally cloud-free skies. In this concept, a cluster of three autonomous stations no more than a few hundred kilometers apart is envisioned for each of the selected regions. This distance is necessary to insure that each station is located in unique weather cell. For a major portion of the time, the spacecraft points to only one of these clusters, handing-off the signal beam to the next cluster as it rises sufficiently above the horizon. Since the intra-cluster distances between stations is of the order of a few hundred km, cloud cover data with much finer spatial resolution (a few tens of km) compared to the LDOS configuration is required. In addition, requirements on the need to obtain site specific cloud cover data with sufficient temporal resolution discussed previously apply here as well,

An advantage of the COS concept over the LDOS is that there is no need to predict weather availability several hours in advance. All stations within the cluster monitor the user transmitted beam jointly with little pointing loss. Additionally, there is no need to designate a receiving station and, therefore, no need to uplink such information to the user spacecraft.

**4.4.2.1 COS with 3x3 Stations.** The clustered optical subnet to be discussed in detail consists of 9 stations located in three clusters of three stations (COS 3x3) approximately 120 degrees apart (~14000 km). This configuration provides 96% user availability by locating stations within a cluster no more than a few hundred kilometers apart.

Ideal coverage curves to model a COS with three clusters of three stations each (COS 3x3) with locations 120° apart in longitude are seen as a subset of the curves for the LDOS configuration with six stations shown in Fig.8 (Consider curves 1a, 3, 5, and 1b only). The assumptions on the sites are the same as described for the LDOS with six stations above, however, it is assumed that only one site in the cluster is receiving telemetry. The availability of this configuration is 96% and the telemetry line is at  $\zeta=60^\circ$  zenith angle, when the handed over to the following cluster takes place.

The geographical cluster locations chosen for the COS 3x3 are shown in Fig. 10. Table 3 provides a list of the specific geographical sites and their weather statistics. Similar to the LDOS network, the data shows that each COS 3x3 site has at least 66% cloud free days. In this configuration each cluster is dedicated to a single user pass resulting in a 96% probability that at least one optical station will have a clear LOS to the user.

Table 3  
Clustered Optical Subnet Locations. The network consists of three ground optical receiving stations in each of the three clusters

	Location	Altitude km	Longitude	Latitude	Time Zone	cloud free days/ Weather	Notes
1	SouthWest United States						
	a. Table Mt. Facility, Ca.	2.3	118 W	34 N	-8	66%/dry[1]	[3]
	b. Mt. Lemmon, Az	2.1	111 W	31 N	-7	>60%/dry[2]	[3]
	c. Sacramento Peak, NM	3.0	106 w	35 N	-7	>60%/dry[2]	[3]
2	Australia						
	a. Freeling Heights[5]	1.1	139 E	30 s	+10	n.a./dry	[4]
	b. Mt. Round	1.6	153E	30 s	+10	n.a.	[4]
	c. Siding Spring Mt.	1.1	149 E	31 s	+10	67%/dry[1]	[3]
3	Spain/NorthWest Africa						
	a. Arin Ayachi, Morocco	3.7	SW	33 N	0	n.a.	[4]
	b. Tahat, Algeria	2.9	5W	22 N	-1	n.a.	[4]
	c. Calar Alto, Spain	2.2	2W	37 N	-1	67%/dry[1]	[3]

[1] ISCCP satellite data; [2] The NOAO 8-M Telescopes proposal to NSF; [3] Precexisting facilities and infrastructure; [4] Information on infrastructure and facilities not available; [5] A. Rogers, personal communication, ANU, Mt. Stromolo and Siding Spring Observatories, Australia, June 1993,

Fig. 11 shows the coverage curves for the COS 3x3 stations when data on **one of the** three actual geographical sites in a cluster is used for a Pluto mission in 2015. The actual sites used to obtain the **coverage** curves are TMF in California, Siding Spring Mt. in Australia, and **Calar** Alto in Spain. The site specific information used to obtain these curves includes altitude, longitude, latitude, as **well** as Pluto's trajectory across the sky. Note that Pluto does **not** pass through the zenith for any of the sites.

In this scenario, as was true for the LDOS configuration discussed above, the characteristic performance of the optical charm] at approximately 70 degrees off **zenith** (handover) is the determining factor for telemetry **performance**. The telemetry curve for the Pluto mission is placed at -6.2 dB compared to -4.7 dB for the ideal case. However, even with this change, two gaps exist in the LOS **coverage** totaling **about 4 hours per day**. The **coverage** provided by the COS 3x3 for a Pluto mission in 2015 is about **79%**. Similar to the LDOS concept each optical terminal has about 20 minutes to acquire, track and lock onto the incoming optical beam. The total network availability has **not** changed, since each cluster contains three sites in **independent** weather cells.

Although this configuration provides the same **telemetry** rate and somewhat better weather availability compared to the LDOS network with 6 stations, the gaps in coverage and the significantly larger number of stations required for the **clustered** concept **are** distinct disadvantages.

**4.4.2.2 COS With 3x4 Stations.** A total of 12 optical stations will be necessary in this configuration of the **subnet** (COS 3x4). The **distance between** clusters will be roughly 90° in longitude (-10000 km), and in the idealized case, the **telemetry** will be handed over to the following cluster at 45° zenith angle. Each cluster (numbered **1** to 4) contains three optical station sites, satisfying the ground rules for the COS concept discussed above.

#### 4.4.3 Network Availability

Weather related availabilities for the **idealized** network configurations are shown in the second column of Table 4. The probabilities have been calculated using the model described above with **q=0.34** for each individual site. Additionally, the acceptable zenith angle loss or the telemetry line used to calculate availabilities for the ideal LDOS networks **are** consistent with a 60° zenith angle and the link calculations shown in **Sec.4.5** below are based on this assumption. Telemetry line, however, can be made consistent with a 75° zenith angle to increase network availability to 92,95, and 96 **percent** for LDOS with 6,7, and 8 stations **respectively**. The trade-off to identify optimum position for the **telemetry** line was not performed.

**Table 4**  
**Network Weather Availability**

Network	Availability for IdCal Sites, percent	Availability for actual Sites, percent
Cos 3x3	96	96
Cos 3x4	96	96
LDOS: 6 stations	88	81
LDOS: 7 station		
LDOS: 8 stations	94	

For actual LDOS with 6 stations for the Pluto mission, a **telemetry** line at 70° zenith angle was used to calculate the network availability as **well** as the data rates shown in **Sec.4.5**. The weather availability for the specific Pluto mission for LDOS with six stations and for a COS with three clusters of three stations each is shown in the third column in Table 4.

#### 4.4.4. Network Coverage

Table 5 shows that the LOS coverage for all idealized optical **subnet** configurations considered here is **100%**. The coverage numbers for the actual geographical sites chosen for LDOS with six stations and COS 3x3 for a Pluto mission in **2015** are shown in the third column of the same table. Note that the coverage for the COS 3x3 for this specific case

drops to 79%. The LOS coverage for COS 3x4 and LDOS with 7 or 8 stations considering actual sites was not calculated but is **expected** to be 100%.

**Table 5**  
**Network LOS Coverage**

Network	Coverage for Ideal Sites, percent	Coverage for actual Sites, percent
Cos 3x3	100	79
C o s 3 x 4	100	
LDOS: 6 stations	100	95
LDOS: 7 stations	100	
LDOS: 8 stations	100	

#### 4.5 LINK CALCULATIONS

Link analysis for a 30 AU Pluto mission at night was performed using OPTI 4.0, a software package developed in house at JPL (see Appendix A). Details on operational and other parameters used in the communication link budget are shown in Appendix A. The modulation format used with the OPTI software was pulse position modulation (PPM). The alphabet size as shown in is 256. A nominal raw link bit error rate of 0.013 was used. This was reduced to 10<sup>-5</sup> by applying 7/8 Red-Solomon coding. The 7/8 correction was applied to the data rate calculated by OPTI].

#### 4.6 TELEMETRY

The telemetry return capability was used as the primary measure of the **subnet** performance. The benchmark established in the study for telemetry is 240 kb/s for a futuristic 70 m **Ka-band receiver averaged** over a 24-hour period. The user spacecraft antenna for this benchmark is 5 m in diameter. The following assumptions and procedures were followed to calculate **telemetry return** capability for optical communications:

- The user spacecraft employs a transmitter **proposed** by TRW for its **DSRSS** study<sup>16</sup>. It is based on a 0.75 m telescope and a 7 W laser operating at 532 nm wavelength. See Appendix A for a list of transmitter parameters **used**.
- Optical terminal is based on a 10 m **telescope**. See Appendix A for a list of **receiver** parameters.
- Data rates for night and day were calculated separately. For the daytime calculation, an average data **rate** was computed over a number of daytime sky radiance values.
- Data rates were computed for an ideal optical **subnet** and a realistic network for a 30 AU mission to Pluto in 2015.
- Data rates were computed for a conventional filter with a spectral bandwidth of 0.2 nm and an atomic resonance filter with a spectral bandwidth of 0.001 nm.
- Day and night time data rates were averaged over a period of 24 hours for both optical filters mentioned above.
- The numbers for availability and coverage were calculated for the **subnet** as reported in Section 4.4.
- Telemetry improvement over the baseline was calculated.

##### 4.6.1 Telemetry for 30 AU Pluto Mission

Table 6 summarizes the data rates, which have been **corrected** for coding as discussed below, **expected** for an optical communications link between a 0.75 m user transmitter at 30 AU and a 10 m ground station. Data rates were calculated for both an ideal configuration and a specific mission to Pluto in 2015 using an atomic resonance filter (**ARF**) as well as a conventional filter. The daytime data rate was obtained by averaging data rates calculated for six **representative** day sky radiances between 10 and 180 degree solar elongation. The **dB** gain, shown in parenthesis with each data rate, was

calculated over the agreed baseline telemetry rate of 240 kb/s. The data rates were first calculated using OPTI 4.0 for 0.013 bit error rate (**BER**) without coding. This raw data rate was then multiplied by 0.877 to obtain 7/8 Reed-Solomon (R-S) coded data rate with  $10^{-5}$  BER for PPM modulation with an alphabet size  $M=256^{17}$ .

**Table 6,**  
**Nighttime and Daytime Average, Day and Night Average data rates (kb/s), and Average Gain (dB) over Baseline Telemetry for a 10 m receiver on ground with Atomic Resonance Filter (ARF) and Conventional Filters. The user transmitter is at a distance of 30 AU, and has a telescope 0.75 m in size.**

	Ideal LDOS with 6 stations		Actual LDOS with 6 stations for a Pluto mission in 2015	
	ARF Filter (BW 0.001 rim), kb/s (dB gain[1])	Conventional Filter (BW 0.1nm), kb/s (dB gain[1])	ARF Filter (BW 0.001 rim), kb/s (dB gain[1])	Conventional Filter (BW 0.1nm), kb/s (dB gain[1])
<b>Nighttime</b>	1716 (8.5)	1716 (8.5)	1215 (7.0)	1215 (7.0)
<b>Daytime Average[2]</b>	<b>1056 (6.4)</b>	<b>377 (2.0)</b>	<b>774 (5.1)</b>	<b>298 (0.94)</b>
<b>Day/Night Average</b>	1386 (7.6)	1047 (6.4)	994 (6.2)	757 (5.0)

[1] The dB gain is calculated over a baseline telemetry rate of 240 kb/s; [2] This is obtained by averaging data rates calculated for six day sky radiances between 10 and 180 degree solar elongation

Table 6 shows that a ground based optical subnet can provide very high data rates. For the Pluto mission at 30 AU the telemetry rate can be as high as 1716 kb/s, about 8,5 dB higher than the baseline rate of 240 kb/s. Daytime data rates are lower as expected, but still provide improvement over the baseline performance.

The telemetry rate can be further improved by employing 12 to 15 m receiver apertures. The technology for photon buckets up to 15 m in size is within reach with low technical risk. Use of a larger aperture, for a given data rate, is expected to have a favorable impact on the user spacecraft design. It will usually mean a user spacecraft optical terminal with smaller mass, size, and power consumption.

## 5. CONCLUSION

Several alternative optical subnet configurations were considered in this article. It is seen that an LDOS with six stations can provide nearly full LOS coverage of the ecliptic and 81 % weather availability. If higher availabilities are needed (up to 96%), an LDOS with 7 or 8 stations can be used.

COS 3x3 under realistic conditions fails to provide full coverage (-79%). If the clustered concept for the optical subnet is desirable, a COS 3x4 will be required with 12 ground stations to provide full coverage, at least for the Pluto mission in 2015. The availability of both COS configurations is expected to be 96%. The COS configuration imposes an additional requirement on locating appropriate specific sites as compared to the LDOS configuration. The clusters must be about ninety degrees apart for COS3X4 longitudinally and additionally intra-cluster station distances must be at least 150 km to ensure decorrelation of weather statistics. It maybe more difficult to find three specific sites within a given cluster when other requirements such as high altitude and reasonable accessibility are included.

A linearly dispersed optical subnet with 6 stations is recommended since it accomplishes the task with fewer ground stations than any other configuration considered in this article.

## Appendix A OPTI SAMPLE OUTPUT

OPTICAL COMMUNICATIONS LINK ANALYSIS PROGRAM, VERSION 4.02  
GBATS, 30 AU, nighttime, 70° zenith angle, ARF spectral filter, PPM, Direct Detection, PMT detector

The transmitter parameters are (user spacecraft):

Transmitter average power (W) = 7.0000  
Wavelength of laser light (micrometers) = 0.53200  
Transmitter antenna diameter (m) = 0.75000  
Transmitter obscuration diameter (m) = 0.00000  
Transmitter optics efficiency = 0.80000  
Transmitter pointing bias error (microrad.) = 0.10000  
Transmitter rms pointing jitter (microrad.) = 0.10000  
Modulation extinction ratio = 0.1E+06

Laser output power (w) 7.00 38.5 dBm  
Min Req'd peak power (W)= 0.4E+04  
Transmitter antenna gain 0.16E+14 132.0  
Antenna dia. (m) =0.750  
Obscuration dia.(m) =0.000  
Beam width (microrad.)=1.121  
Transmitter optics efficiency 0.800 1.0  
Transmitter pointing efficiency 0.893 -0.5  
Bias error (microrad.)=0.100  
RMS jitter (microrad.)=0.100

The receiver parameters are (ground station):

Diameter of receiver aperture (m) = 10.000  
Obscuration diameter of receiver (m) = 3.0000  
Receiver optics efficiency = 0.70000  
Detector quantum efficiency = 0.21000  
Narrowband filter transmission factor = 0.60000  
Filter spectral bandwidth (angstroms) = 0.1E-01  
Detector dia. field of view (microrad.) = 10000

Space loss ( 30.00 AU ) 0.89E-40 -400.5  
Receiver antenna gain 0.45E+16 156.5  
Antenna dia. (m) =10.0  
Obscuration dia. (m) =3.0  
Field of view (microrad.)=100.0  
Receiver optics efficiency 0.700 -1.5  
Narrowband filter transmission 0.600 -2.2  
Bandwidth (angstroms) =0.01  
Detector Quantum efficiency 0.210 -6.8

The operational parameters are:

Alphabet size (M = ?) = 256.00  
Data rate (kb/s) = 1387.8  
Link distance (A.U.) = 30.000  
Required link bit error rate = 0.13E-01  
Atmospheric transmission factor = 0.24000  
Dead time (microseconds) = 3.2046  
Slot width (nanoseconds) = 10.000

Atmospheric transmission factor 0.240 -6.2  
Received signal power (W) 0.23E-11 -86.4 dBm  
Recv'd background power (w) =0.32E-17  
Photons/joule 0.27E+19 154.3 dB/mJ

Detected signal PE/second 0.26E+07 64.1 dBHz  
Symbol time (seconds) 0.29E-05 -55.4 dB/Hz

Detected signal PE/symbol 7.36 8.7  
Required signal PE/symbol 3.69 5.7  
Detected background PE/slot= 0.74E-04

Noise sources

Pluto RCVR to source distance (AU) = 30.000  
nightsky radiance(W/M\*\*2/SR/A) = .5E-08

Margin 2.00 3.0

## Appendix B Site Selection Guidelines and Procedure

### B.] SELECTION GUIDELINES

The following guidelines were used to identify probable sites for the earth based optical communication terminals:

- a. Locations as close to equator as possible
- b. High altitudes, preferably mountain tops
- c. Good astronomical seeing
- d. Large number of cloud free days per year
- e. Accessible locations with existing infrastructure if possible

### B.2 SELECTION PROCEDURE

To start, large geographical regions with appropriate distance in longitude between them for the network configuration under consideration, and as close to the equator as possible were identified on a map. A detailed literature search was then performed to locate sites at high altitudes in each region, thus generating a large list of likely station sites. Sites with good astronomical seeing, large number of cloud free days, and preexisting infrastructure were favored, Inaccessible sites with wet weather were dropped from consideration when better alternates were available.

### B.3 LIST OF ADDITIONAL POSSIBLE SITES

Table B-1 provides a list of geographical sites in addition to those already listed in the body of the report. Each possible site in this table, and the site tables shown elsewhere in this report is followed by its altitude, longitude, latitude, and the time zone. The next column provides information on the number of cloud free days and the weather of the site. The cloud cover data on most sites were obtained from the International Satellite Cloud Coverage Project (ISCCP) as managed by the NASA Climate Data System (NCDS) and available on CD-ROM<sup>18</sup>. The data provides monthly averages over an 8 year period ending in Dec., 1990 for the entire globe with a resolution of 250 km<sup>19</sup>. Data on other sites like Mauna Kea in Hawaii were obtained *in situ* for astronomical purposes. The last column indicates if there is preexisting infrastructure at the site.

**Table B-1  
Additional sites of interest to an optical communications network**

Location	Altitude km	Longi- tude	Latitude	Time Zone	cloud free days/ Weather	Notes
Roque de 10S Muchachos Obser., Canary Is., Spain	n.a.	16W	29 N	-2	n.a./dry	[3]
Fuente Nueva, La Palma, Canary Is., Spain	n.a.	16W	29 N	-2	n.a./dry	[3]
Jabal Toukal, Morocco	4.1	8W	31 N	0	n.a./dry	[4]
Mulhccen, Spain	3.4	3W	37 N	-1	67%/dry [1]	[4]
Inafia, Tenerife, Canary Is., Spain	n.a.	16 W	29 N	-2	n.a./dry	[3]
Cerro Tololo, Chile	2.2	71W	30 s	-4	77%/arid [2]	[3]
Llano del Hato, Venezuela	3.6	71 w	9 N	-4	n.a./dry	[3]
Mt. Ziel, Australia	1.5	133 E	23 S	10	n.a./dry	[4]

[1] ISCCP satellite data; [2] The NOAO 8-M Telescopes proposal to NSF; [3] Preexisting facilities and infrastructure; [4] Information on infrastructure and facilities not available.

## 6. REFERENCES

- 1 JPL Contract No: 958733 with TRW and JPL Contract No: 958734 to **STEL, Jet Propulsion Laboratory**, Pasadena, CA, March 28, 1990.
- 2 **K. Shaik**, D. Wonica, and M. Wilhelm, "Optical **Subnet** Concepts for the Deep Space Network," TDA Progress Report, 42-115, pp.153-81, 1993.
- 3 **K. Shaik**, "progress on **ten-meter** optical **receiver telescope**," SPIE vol. 1635, Ed. David L. Begley and Bernard D. Seery, pp.109-117, 1992.
- 4 **K. Shaik**, "A Preliminary Weather Model for Optical Communications Through the Atmosphere," TDA progress Report 42-95, pp.212-218, 1988
- 5 **K. Shaik** and J. Churnside, "Laser Communication Through the Atmosphere," Proceedings of the Twelfth NASA Propagation Experimenters Meeting (**Napex XII**), pp.126-131, Jun. 9-10, 1988.
- 6 TRW Briefing "**Deep** Space Relay Satellite System Study," Quarterly progress Review, Presented to JPL on February 25, 1993.
- 7 *ibid.*
- 8 J. Nelson, T. **Mast**, and S. Faber, "The Design of the Keck Observatory and Telescope, p.2-11, Keck Observatory Report No. 90, 1985.
- 9 See ref. 4 above
- 10 **D.P. Wylie** and **W.P. Menzel**, "Cloud cover statistics using VAS," SPIE's OE-LASE'88 Symposium on Innovative Science and Technology, Los Angeles, CA, January 10-15, 1988.
- 11 **K. Shaik**, "Spatial Correlation of **cloud** System s," JPL IOM 331-88,6-564 (internal document), JPL, Pasadena, CA, October 7, 1988
- 12 See ref. 4 above
- 13 The probability of opaque clouds in the S W USA is less than 20 percent, see ref. 4 above.
- 14 **Greenhouse** Effect Detection Experiment (**GEDEX**), 1992 Update, World Data Center for Rockets and Satellites, Code 902.2 DAAC, Goddard Space Flight Center, **Greenbelt**, Md, 1992.
- 15 The NOAO 8 m Telescopes (Now Called Gemini 8 m Telescopes) proposal to National Science Foundation, 1988.
- 16 See ref. 6 above
- 17 W. Marshall, "Using the Link Analysis Program with R-S encoded Links," JPL IOM 331 -86.6-202 (internal document), JPL, Pasadena, CA, August 1, 1986.
- 18 **Greenhouse** Effect Detection Experiment (**GEDEX**), 1992 Update, World Data Center for Rockets and Satellites, Code 902.2 DAAC, Goddard Space Flight Center, **Greenbelt**, MD, 1992.
- 19 **K. Shaik** and D. **Wonica**, "Cloud Cover Data for **GBATS**," JPL IOM 331.6-93-098 (internal document), JPL, Pasadena, CA, May 6, 1993.

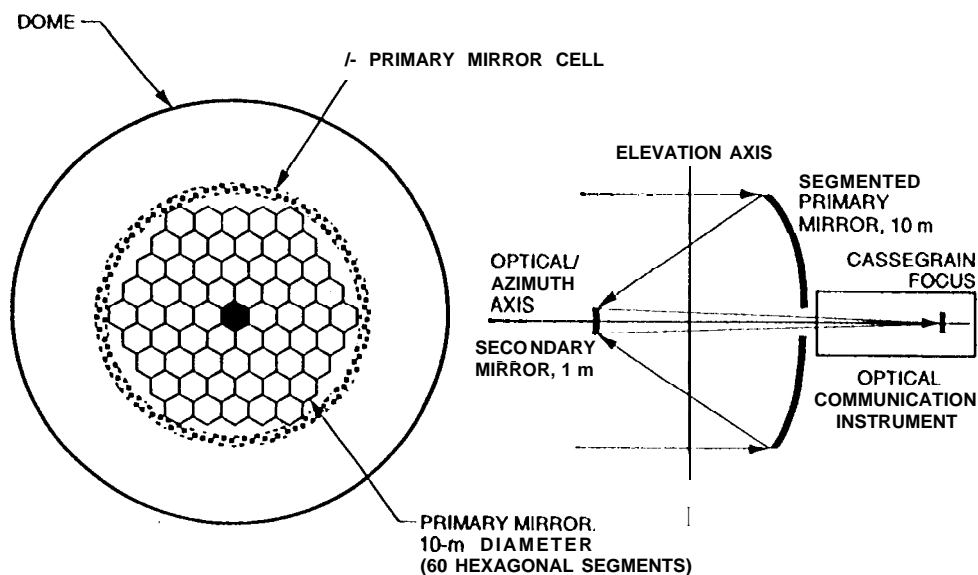


**Fig.1.** Conceptual diagram of the 10 m telescope for the ground optical terminal. (not drawn to scale). Primary diameter = 10 m; FOV at Cassegrain focus = 2.0 mrad; coarse pointing accuracy = 0.2 mrad; blur diameter at focus  $\leq 0.1$  mrad; and the fine pointing accuracy = 0.01 mrad.

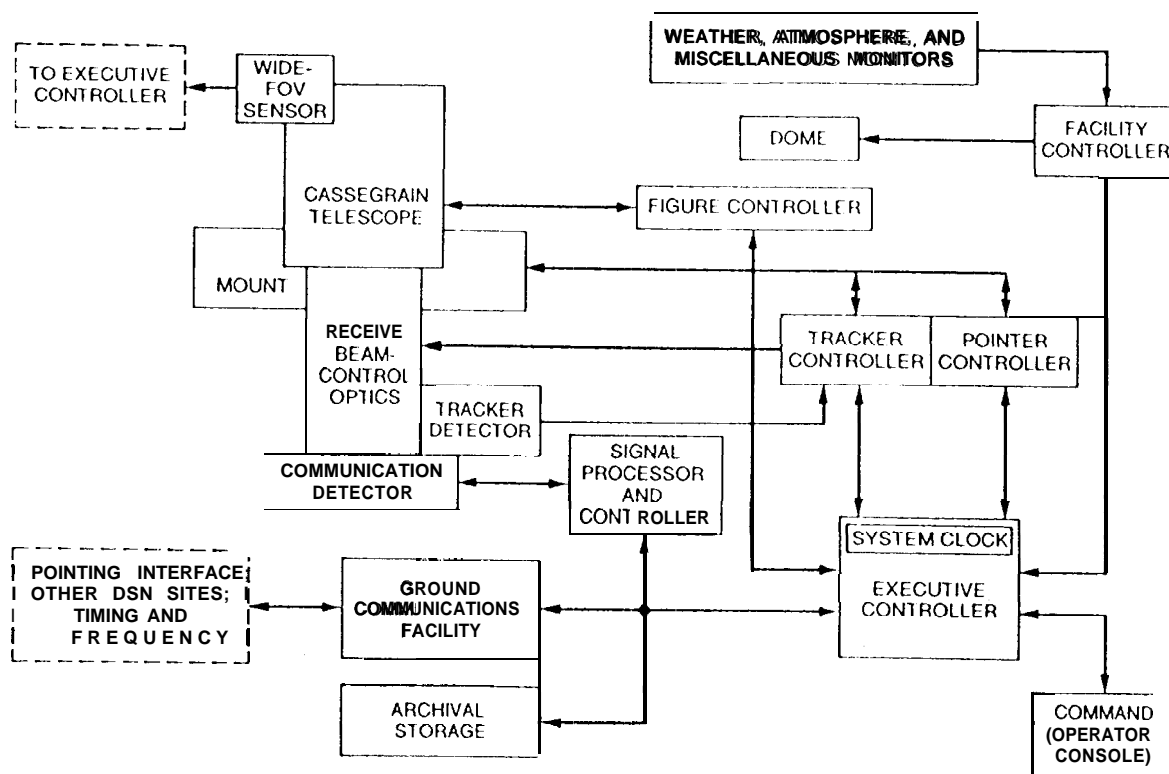


**Fig.2.** Ground optical station block diagram,



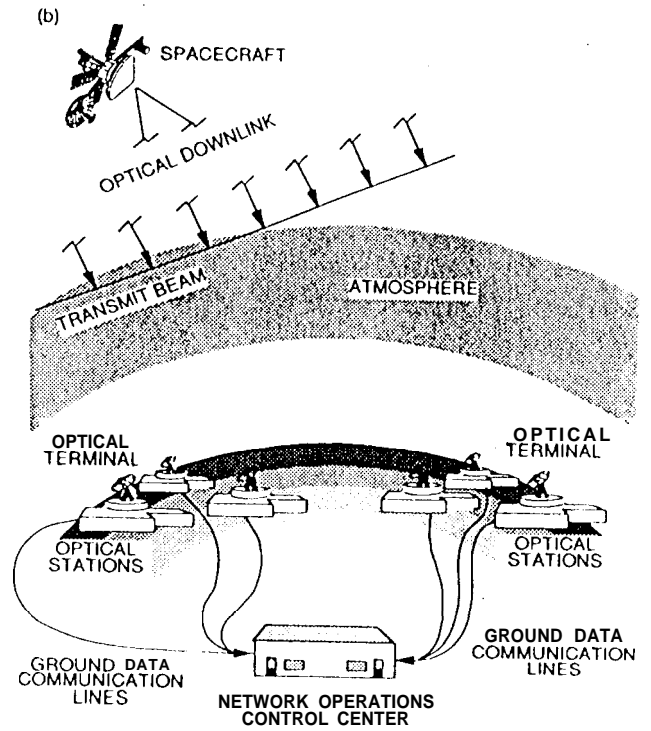
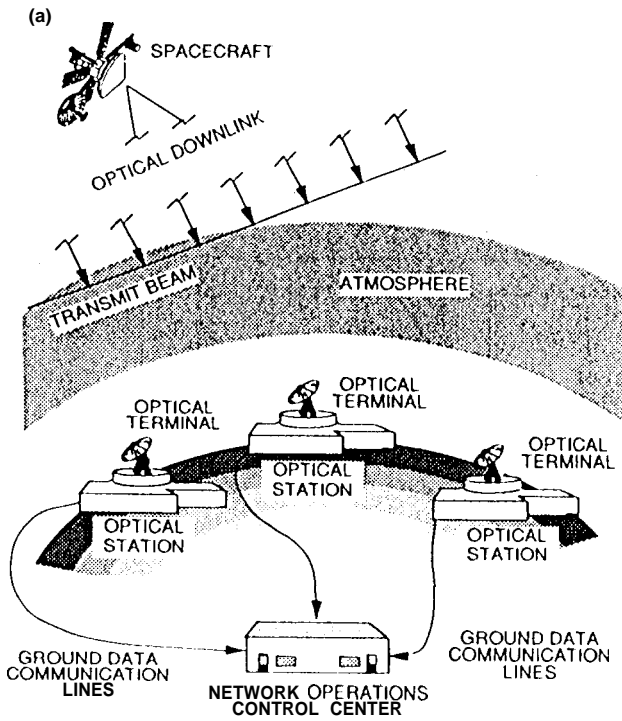
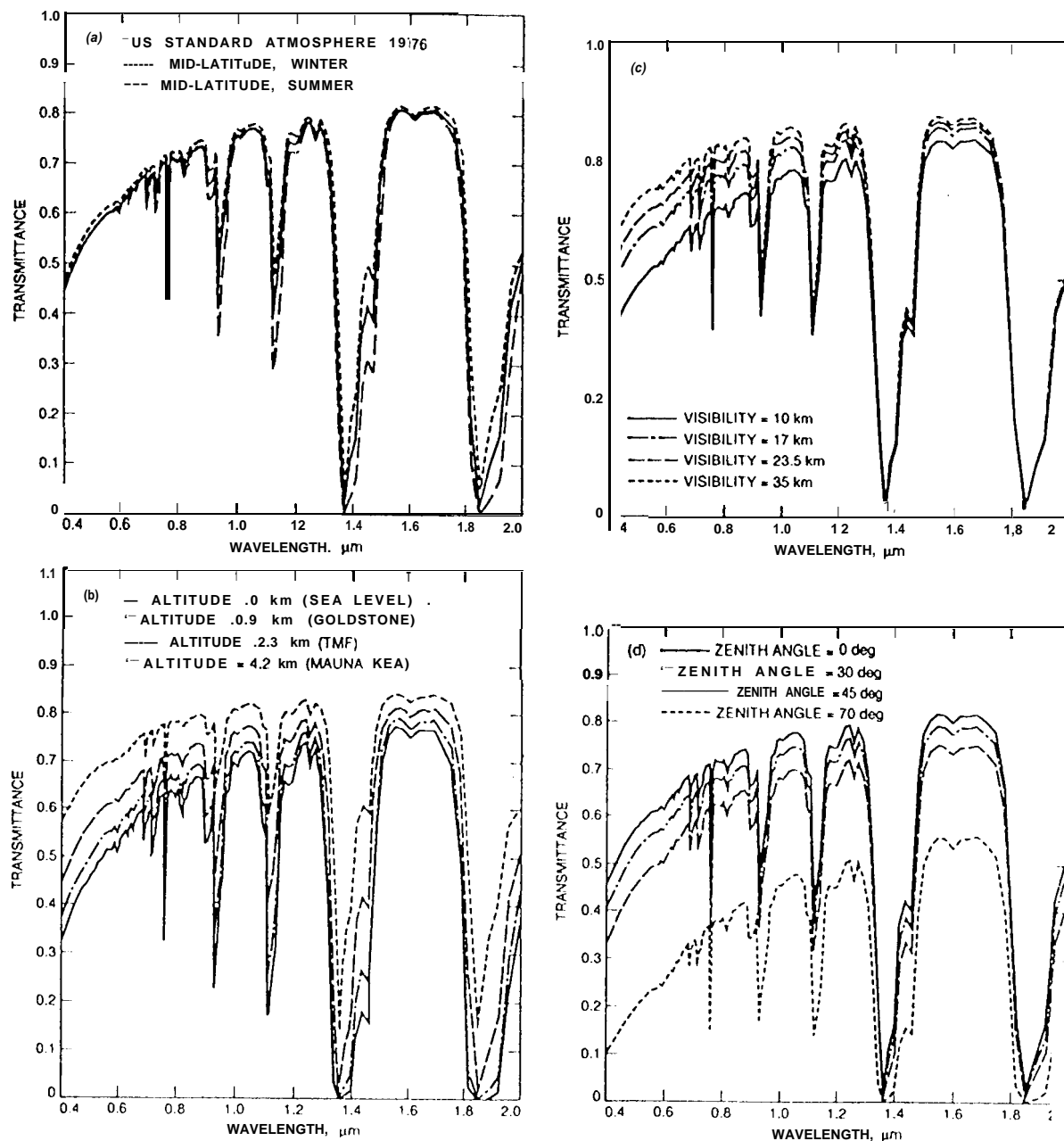


Fig.3. Network Geometry (not drawn to scale): (a) LDOS, (b) COS



**Fig.4. Spectral transmittance data.** (a) Spectral transmittance over visible and near infrared wavelengths for three LOWTRAN atmospheric models. Assumes high cirrus clouds, a 2.3 km altitude, a 17 km meteorological range (clear), and zenith path through the atmosphere. (b) Spectral transmittance for selected altitudes over visible and near infrared wavelengths. Assumes US Standard 1976 atmosphere with high cirrus clouds, a 17 km meteorological range (clear), and zenith path through the atmosphere. (c) Spectral transmittance for selected meteorological ranges (visibilities) over visible and near infrared wavelengths. Assumes US Standard 1976 atmosphere with high cirrus clouds, a 2.3 km altitude, and a zenith path through the atmosphere. (d) Spectral transmittance for selected zenith angles over visible and near infrared wavelengths. Assumes US Standard 1976 atmosphere with high cirrus clouds, 2.3 km altitude, a 17 km meteorological range (clear), and a path through the atmosphere.

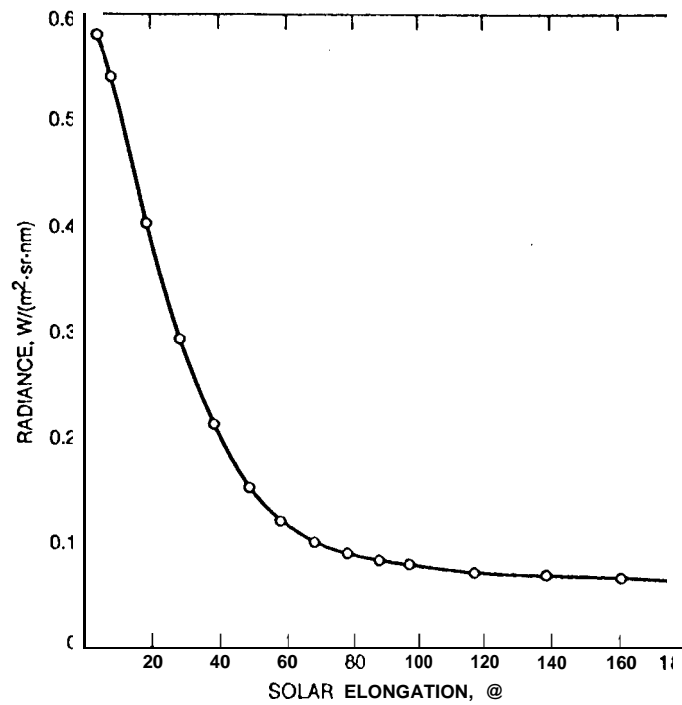


Fig.5. Daytime sky radiance as a function of solar elongation (sun-earth-probe angle).

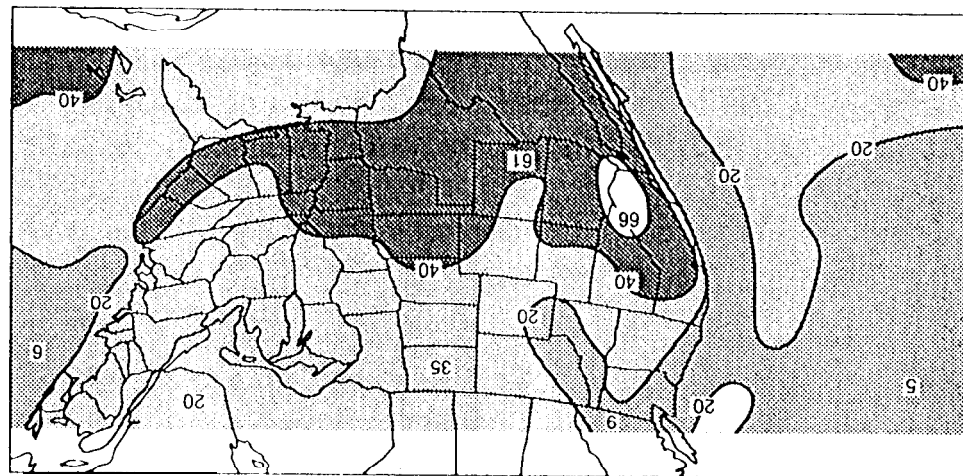


Fig.6. Contour diagram obtained from 2 years of GOES satellite data showing the probability of clear skies over the United States (see ref. 10).

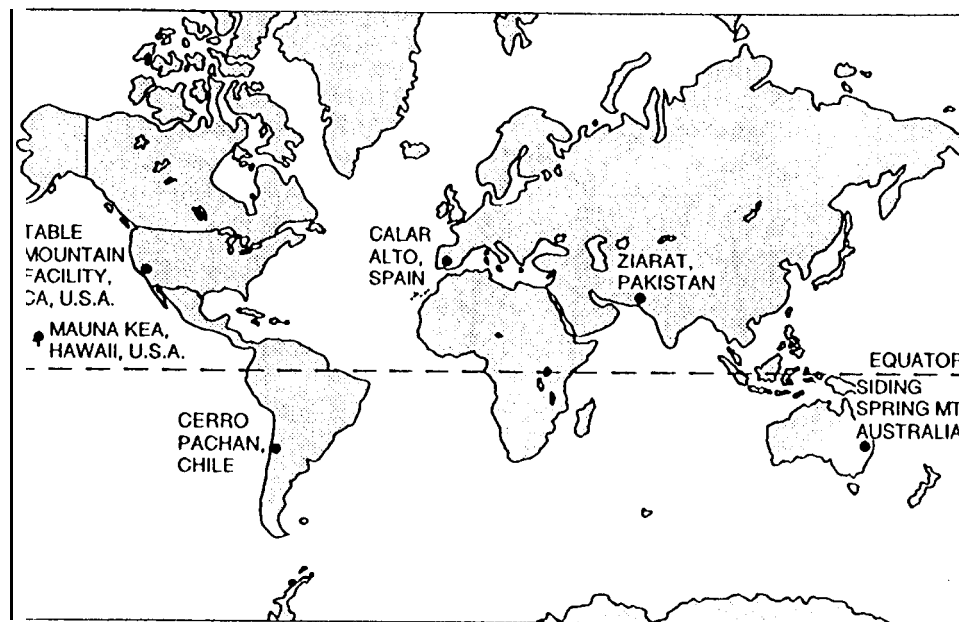


Fig.7. Geographical sites for LDOS with six stations.

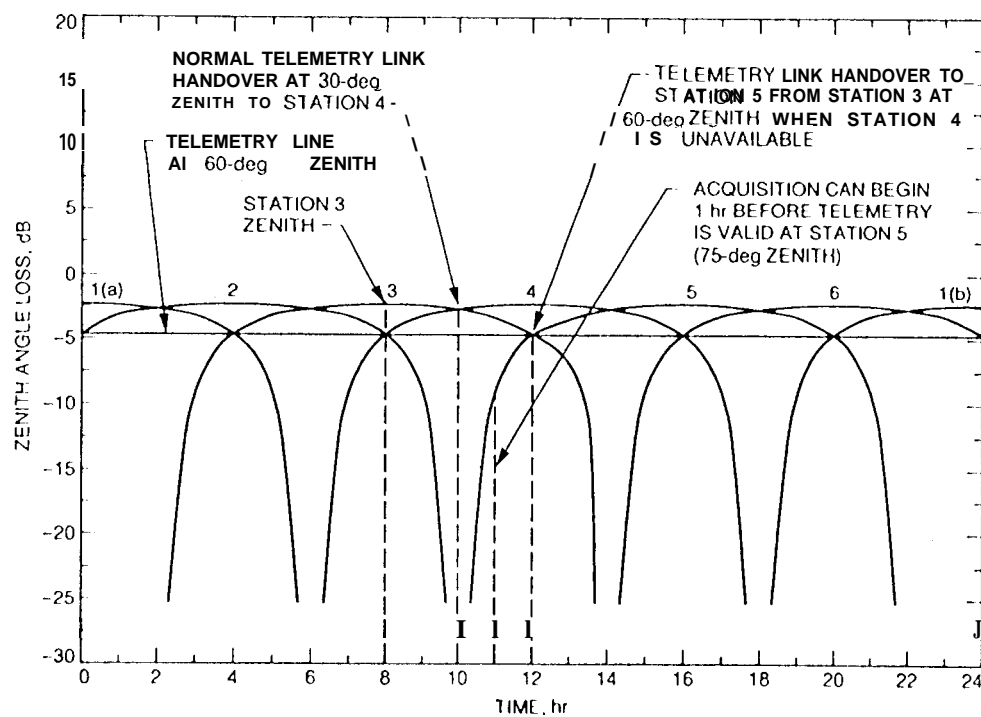


Fig.8. Ideal coverage curves over one day for an LDOS subnet with six stations sixty degrees separation in longitude in an equatorial belt.

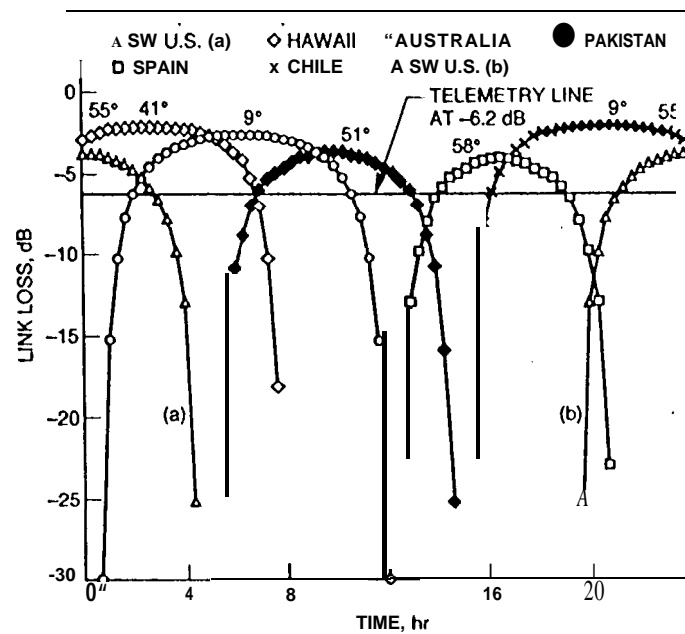


Fig.9. Coverage curves for six actual sites for a Pluto link in 2015. Zenith angles at local meridian for Pluto in 2015 are shown at the top of each curve. The sites used are shown in Table 2. The coverage curve for SW US is shown in two halves: SW US (a) and SW US (b).

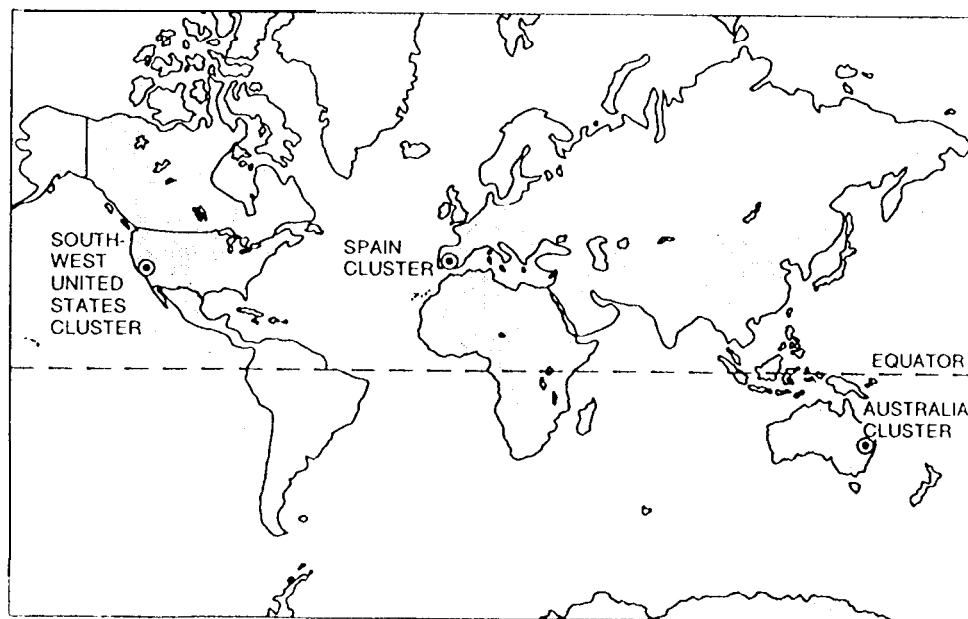
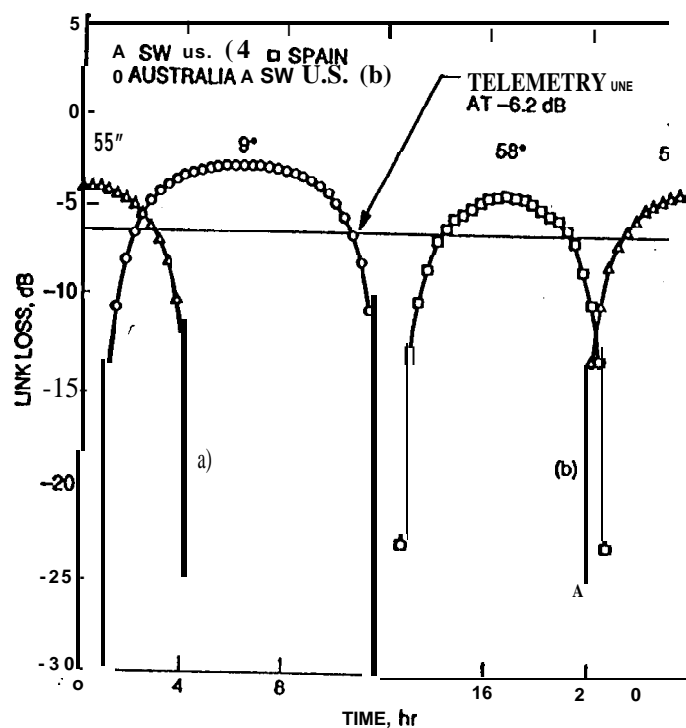


Fig.10. Geographical sites for COS3x3 Subnet



**Fig.11.** Coverage curves for a COS 3x3 with nine stations for a Pluto mission in 2015. Zenith angles at local meridian for Pluto in 2015 are shown at the top of each curve. The sites used to calculate the coverage curves are TMF in California, Siding Spring Mt. Australia, and Calar Alto in Spain (see Table 3). The Coverage curve for SW US is shown in two halves: SW US (a) and SW US (b).